

# RESEARCH ON URBAN SURFACE EMISSIVITY BASED ON UNMIXING PIXEL

D. Q. Peng, Y. H. Chen\*, J. Li, J. Zhou, W. Ma

State Key Laboratory of Earth Surface Processes and Resource Ecology (Beijing Normal University), College of Resources Science & Technology, Beijing Normal University, Beijing 100875, China,

\* Corresponding author: - cyh@ires.cn

**KEY WORDS:** Remote Sensing, Urban, Algorithm, Infrared, Estimation

## ABSTRACT:

Surface emissivity is a measure of inherent efficiency of land surface. It is applied to convert heat energy into radiant energy. In this study, an unmixing pixel based algorithm was proposed to compute pixel effective emissivity for Advanced Spaceborne Thermal Emission and Reflection Radiometer (ASTER) data within Beijing, China. In this paper, vegetation, together with water and 3 kinds of manmade materials surface distribution is estimated through a part constrained linear spectral model after PPI (Purity Pixel Indices) calculated. Sample emissivities presented in this research were extracted from Jet propulsion laboratory (JPL) spectral database. Root Mean Square Error (RSME) results of the whole study area is 0.1012, 0.0952, 0.2178, 0.0941 and 0.0951 for ASTER 5 TIR (8.125~11.65 $\mu$ m) bands, respectively. This study suggests that this model is useful for the estimation of land surface emissivity, and it can be used as a rather simple alternative to complex algorithms.

## 1. INTRODUCTION

Surface emissivity is an important parameter for studies of global energy balance. Thus estimation of emissivity is of particular interest.

A number of methods have been explored in order to retrieve land surface emissivity, such as Temperature-Independent Spectral Indices (TISI) methods (Tian et al., 2006). Some TISI methods are described in Becker and Li (Li & Becker, 1993; Becker & Li, 1995). This kind of algorithm combines middle wave infrared data (MWIR: 3.4-5.2 $\mu$ m) with thermal infrared data (TIR: 8-14 $\mu$ m) to measure emissivity. Gilleapie et al. (1998) developed this method for ASTER data and carried out a high accuracy results. But the accuracy of this algorithm depends on some assumptions and ties to atmosphere correction. NDVI methods proposed by Caselles et al. (1989) and developed by Van et al. (1993) supply a new technique to calculate emissivity, and performance successfully in natural surface. But this method assumes the land surface is mainly made up of two types-vegetations and soil, which is disagreement with urban surface. Wan et al. (1998) utilized classification-based emissivity method and applied results to split window method, which performed well and the accuracy of land surface temperature is  $\pm 1K$  (1996). Snyder et al. (1990) also used this method to retrieval global emissivity without considering the complicated urban surface.

Urban surface is more complex. And spectral heterogeneity is notable due to the spatial resolution, especially for TIR image. So it is common for the existence of mixing pixel. And effective emissivity should be given more attention. This study utilizes Linear Spectral Mixture Analysis (LSMA) and spectral database to extract subpixel information and achieve pixel effective emissivity.

## 2. METHOD

### 2.1 Study Area and Data Processing

Study area is located in Beijing city (Fig.1). Beijing, a metropolitan city, is a centre of China. Urbanization is continuing to accelerate in this megacity. The pattern of it is complex and pixel mixing phenomenon is outstanding. The selected region contains most of representation urban land features, including vegetation, water, central business distinct, and so on.

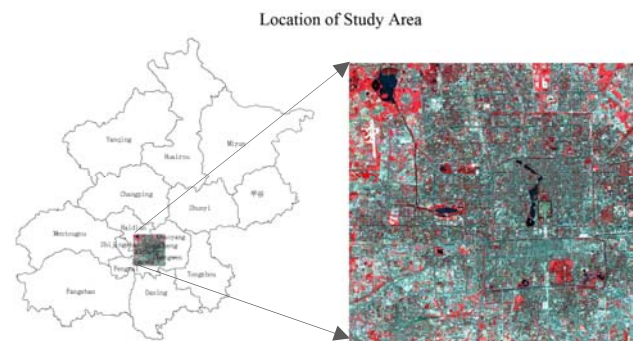


Figure 1. Location of study area

Advanced Spaceborne Thermal Emission and Reflection Radiometer (ASTER) L1B Metadata and L2B emissivity product data acquired on 31<sup>st</sup> August 2004 is used in this study. ASTER provides images in Visible/Near-Infrared (VNIR) with a spatial resolution of 15m, in Shortwave-Infrared (SWIR) with a spatial resolution of 30m, and in TIR with a resolution of 90m (Abrams, 2000; Yamaguchi et al., 1998). Hence, it is more suitable for urban studies at region scales than other satellite data, such as the Moderate Resolution Imaging Spectroradiometer (MODIS), which has a resolution of 250m, 500m, 1000m for VNIR, SWIR and TIR, respectively (Lu et al., 2006).

ASTER emissivity product is obtained using a hybridized algorithm (<http://asterweb.jpl.nasa.gov/documents.asp>). This method first should estimate temperature and band emissivities by Normalized Emissivity method. And then the value calculated in the first step is normalized using a ratio-method. Next, Min-Max Difference approach is utilized to predict the minimum emissivity according experience equation. After several iterative calculations, emissivity product is acquired. This product accuracy is  $\pm 0.015$ . So it will perform well in many applications.

Atmosphere correction and radiant correction has been done for L1B metadata, but without geometric correction. Because ASTER metadata contains Geometric Correction Tables (GCTs) for each telescope, geometric rectify can also be done according to a file published on March 31, 2006 ([http://lpdaac.usgs.gov/aster/ASTER\\_GeoRef\\_FINAL.pdf](http://lpdaac.usgs.gov/aster/ASTER_GeoRef_FINAL.pdf)).

## 2.2 Spectral Unmixing

Owing to low spatial resolution of TIR data, mixing pixel problem will be encountered in any research, especially in urban area. Mao et al. (2007) assumed land surface is consisted of soil, vegetation, water and rocks. Ridd (1995) proposed a V-I-S (Vegetation-Impervious-Soil) model aiming at urban centre and suburb. In this research, study area lies in city centre, where vegetation, water and manmade-surface (included concrete surface, road, and residential area) have a high proportion and the proportion of soil is small. Thus in this study, urban surface consists of vegetation, water and manmade materials.

In this study, part constrain line spectral mixture model is applied to unmix spectral. Line spectral mixture model is a technique to extract subpixel information, based on the assumption that the spectrum of a pixel is a combination of the spectral of all components within the pixel, and the weight depends on proportion of the area covered by distinct features on the ground (Lu et al., 2006). If there is any scatter between components in a pixel, LSMA can be expressed as the following equation (Yuan & Bauer, 2007):

$$\begin{cases} \rho_b = \sum_{i=1}^n (\rho_{i,b} * f_i) + e_b \\ \sum_{i=1}^n f_i = 1 \end{cases} \quad (1)$$

Where  $\rho_b$ =reflectance of pixel in band  $b$   
 $\rho_{i,b}$ =reflectance of component(endmember)  $i$  in band  $b$   
 $f_i$ =area proportion of endmember  $i$  in a pixel  
 $e_b$ =error of model in band  $b$

The crucial problem for LSMA performing successfully is to select high-quality endmembers (Lu et al., 2006; Zhou et al. 2007). Many methods were developed for endmember selection (Lu et al. 2003). In this research, three kinds of endmembers (water, vegetation, and 3 kind manmade materials) were selected using Image-based approach after Purity Pixel Indices (PPI) calculating. The larger PPI value indicates spectral is more pure (Lu & Lin, 2004; Xia et al., 2004). And then a part constrained least-squares solution is utilized to unmix the spectral image into fractions due to its simplicity and ease of implementation (Smith et al., 1990; Lu et al. 2003).

The fraction result is close to land surface feature distribution. Fig. 2 shows manmade fraction account for a majority in the central business distinct, and the fraction of vegetation is small. In some virescence place, such as in the park, proportion of vegetation is close to 1. In residential area, manmade materials and vegetation is blended owing to execution of environmental planning in the city. Aircraft in suburb has a high proportion of manmade fraction. The white colour in Fig. 2 (a) and (b) is water.

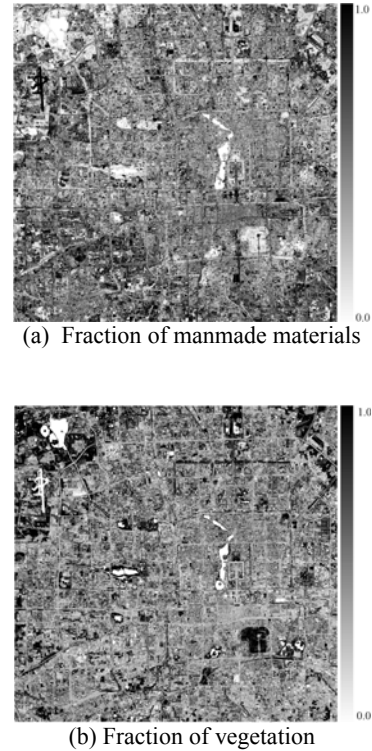


Figure 2. Fraction of land surface in study area

## 2.3 Surface Emissivity Simulation

Land surface emissivity depends on the composition, structure, wetness and observation conditions (i.e., observation wavelength, and angle) (Dozier & Warren, 1982). If there is  $N$  kinds of endmembers in a pixel, assuming temperature of all endmembers is the same, the relationship between endmember fraction and the effective emissivity  $\varepsilon$  in the pixel can be given as (Tian et al., 2006; Chen et al., 2000):

$$\varepsilon = \sum_{i=1}^N \varepsilon_i * f_i \quad (2)$$

Where  $\varepsilon_i$ = emissivity of endmember  $i$   
 $f_i$  = fraction of endmember  $i$  in a pixel

Then pixel effective emissivity  $\varepsilon_b$  in the study area can be shown as:

$$\varepsilon_b = f_v \varepsilon_v + f_m \varepsilon_m + (1 - f_v - f_m) \varepsilon_w \quad (3)$$

Where  $\epsilon_{m,b}$ =manmade material emissivity in band b  
 $f_v$ =fraction of vegetation in a pixel  
 $f_m$ =fraction of vegetation manmade material in a pixel

Many researches prove spectral curve of different vegetation and water is almost same in TIR region (Mao et al., 2007; Nerry et al., 1990; Rubio et al., 1997; Sobrino et al., 2001; Sobrino et al., 2004; Stathopoulou & Cartalis, 2007). In this research, vegetation emissivity  $\epsilon_v$  and water emissivity  $\epsilon_w$  is valued as 0.985 and 0.990, respectively. Manmade land surface emissivity is obtained by using spectral database provided by Jet propulsion laboratory (<http://speclib.jpl.nasa.gov>). After analyzing 46 kinds (including 6 kind concrete materials, 17 kind General Construction Materials, 5 kind Road Asphalts and Tar and 18 kind Roofing Materials) manmade material emissivity (Fig. 3), we utilize mean emissivity of concrete, general construction materials and road asphalts and tar materials in Eq.3. Because central business distinct building and surrounding of it in study area are covered by concrete. And residential is almost constructed by brick. Road is covered by asphalts and tar.

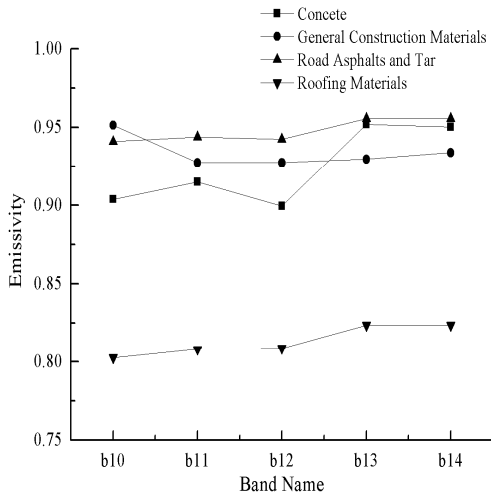


Figure 3. Mean emissivity of manmade sample

### 2.4 Results and Discussion

In order to analyze the emissivity obtained from unmix method, results were resampled to 90m resolution (Fig. 4), and then compared with ASTER emissivity product. Evaluation of this algorithm is done by using RSME (Root Mean Square Error) expressed as equation 4:

$$RMSE_b = \sqrt{\frac{\sum_{m=1}^M \sum_{n=1}^N (\epsilon_{m,n} - \tilde{\epsilon}_{m,n})^2}{m * n - 1}} \quad (4)$$

Where  $RMSE_b$ = Root Mean Square Error of band b  
 $\epsilon_{m,n}$ =emissivity of pixel location at (m,n) baesd on unmixing algorithm  
 $\tilde{\epsilon}_{m,n}$ =ASTER product emissivity of pixel location at (m,n)

Band NO.	Spectral Range (μm)	RMSE
Band10	8.125~8.475	0.101
Band11	8.475~8.825	0.095
Band12	8.925~9.275	0.218
Band13	10.25~10.95	0.094
Band14	10.95~11.65	0.095

Table 1. RMSE of the whole study area

Result shown in Tab.1 indicates our model has a larger RMSE in band 12 and band 10. This maybe because emissivity in 8.925μm~9.275μm and 8.125μm ~8.475μm is much more variable, especial for manmade materials. Sample emissivities in these spectral ranges prove it as Fig. 3 seen:

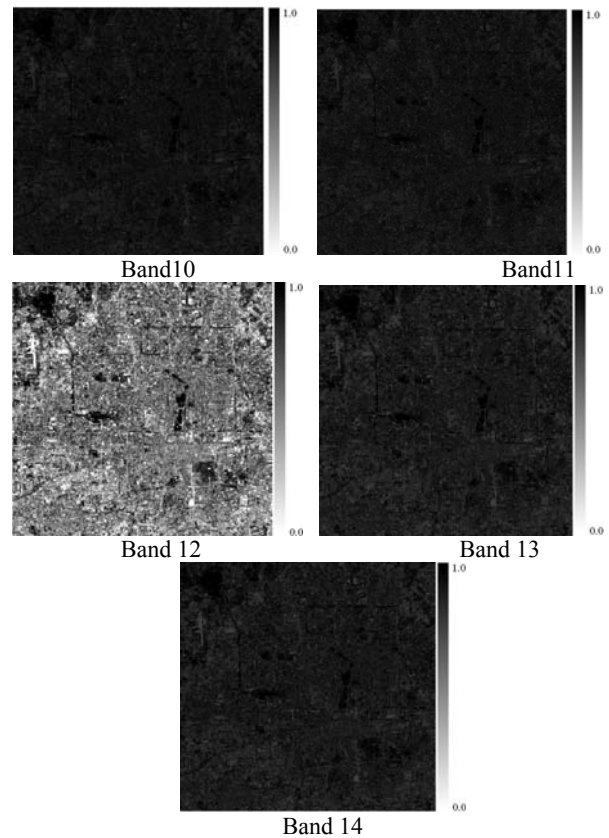


Figure 4. Emissivity results of the model in different band

Assumption of this model can also contribute to RMSE. First, we describe the most suitable condition in a pixel (without scattering between distinct land features and temperature is the same of them). The fact is scattering exists between features and temperature of them is of difference due to their different attributes. Second, just three kinds of manmade materials' (concrete, general construction materials and road asphalts and tar) mean emissivity is utilized in the model. But emissivity of these materials has a range. Third, soil is not in consideration for this algorithm. And it maybe shown in some place, such as constructing area, park, and so on. Last, result of this method depends on LSMA. LSMA is computed by part constrained least-squares approach, leading to fraction of some feature larger than 1 and some lower than 0. When this problem countered, we will make the fraction equal to 1 or to 0, which also can make an error.

### 3. CONCLUSIONS

In this study, we have proposed an unmixing based algorithm to estimate the effective emissivity of a pixel. According to the research, some points were presented.

1. It was validated to calculate effective emissivity using this method. And it is easy to implement. There is two steps to compute emissivity. First, feature fraction in a pixel is extracted thanks to LSMA method. And then is pixel effective emissivity estimation, using a linear equation.

2. Results obtained here come out several issues that would be worth studying in the future:

- (a) Considering scattering between features is better to estimate effective emissivity;
- (b) Introducing heterogeneity of surface for the model;
- (c) Correction of model parameters with feature fraction.

### ACKNOWLEDGEMENTS

Foundation of The Natural Science Foundation of China (40771136,40701114) and the National Basic Research Program of China (2007CB714403, 2006CB701302).

### REFERENCES

Abrams, M., 2000. The Advanced Spaceborne Thermal emission and reflection radiometer (ASTER): data products for high spatial resolution imager on NASA's Terra platform. *International Journal of Remote Sensing*, 21, pp. 847-859.

Becker, F., & Li, Z., 1995. Surface temperature and emissivity at various scale: definition, measurement, and related problem. *Remote Sensing Review*, 12, pp. 225-253.

Caselles, V., & Sobrino, J. A., 1989. Determination of frosts in orange groves from NOAA-9 AVHRR data, *Remote Sensing of Environment*, 29, pp. 135-146.

Chen, L. F., Zhuang, J. L., Xu, X. R., Niu, Z., Zhang, R. H., & Xiang, Y. Q., 2000. The definition and validation of nonisothermal surface's effective emissivity. *Chinese Science Bulletin*, 45(1), pp. 22-29.

Coll, C., Caselles, V., Valor, E., Niclòs, R., Juan, M., Joan, M., & Mira, M., 2007. Temperature and emissivity separation from ASTER data for low spectral contrast surfaces. *Remote Sensing of Environment*, 110, pp. 162-175.

Dozier, J., & Warren, S. G., 1982. Effect of viewing angle on the infrared brightness temperature of snow. *Water Resource Research*, 18, pp. 1424-1434.

Gillespie, A., Rokugawa, S. I., Matsunaga, T., Cothorn, J. S., Hook, S., & Kahle, A., 1998. A temperature and emissivity separation algorithm for Advanced Spaceborne Thermal Emission and Reflection Radiometer (ASTER) images. *IEEE Transaction on Geoscience and Remote Sensing*, 36, pp.1113-1126.

Li, Z. L., & Becker, F., 1993. Feasibility of land surface temperature and emissivity determination from AVHRR data. *Remote Sensing of Environment*, 43, pp. 67-85.

Lu, D., & Weng, Q., 2006. Spectral mixture analysis of ASTER images for examining the relationship between urban

thermal features and biophysical descriptors in Indianapolis, Indiana, USA. *Remote Sensing of Environment*, 104, pp. 157-167.

Lu, D., Moran, E., & Batisetella, M., 2003. Linear mixture model applied to Amazonian vegetation classification. *Remote Sensing of Environment*, 87, pp. 456-469.

Lu, D., & Weng, Q., 2006. Spectral mixture analysis of ASTER images for examining the relationship between urban thermal features and biophysical descriptors in Indianapolis, Indiana, USA. *Remote Sensing of Environment*, 104, pp. 157-167.

Lu, Y., & Lin, N., 2004. Macroscopic assessment of land degradation in Songliao plain using MODIS data. *Geography and Geo-Information Science*, 20(3), pp. 22-25.

Mao, K., Shi, J., Li, Z., & Tang, H., 2007. An RM-NN algorithm for retrieving land surface temperature from EOS/MODIS data. *Journal of Geophysical Research*. 112, pp. 1-17.

Nerry, F., Labeled, J., & Stoll, M. P., 1990. Spectral properties of land surface averaged emissivity measurements. *Journal of Geophysical Research*, 95(B5), pp. 7072-7044.

Ridd, M. K., 1995. Exploring a V-I-S (vegetation-impervious surface- soil) model for urban ecosystem analysis through remote sensing: comparative anatomy for cities. *International Journal of Remote Sensing*, 16, pp. 2165-2185.

Rubio, E., Caselles, V., & Badenass, C., 1997. Emissivity measurements of several soils and vegetation types in the 8-14 $\mu$ m waveband: Analysis of two field methods. *Remote Sensing of Environment*, 59, pp. 490-521.

Smith, M. O., Ustin, S. L., Adams, J. B., & Gillespie, A. R., 1990. Vegetation in Deserts: I. A regional measure of abundance from multispectral images. *Remote Sensing of Environment*, 31, pp. 1-26.

Sobrino, J. A., Raissouni, N., & Li, Z. L., 2001. A comparative study of land surface emissivity retrieval from NOAA data. *Remote Sensing of Environment*, 75, pp. 255-267.

Sobrino, A., Juan, C., Jiménez-Muñoz, Leonardo Paolinib, 2004. Land surface temperature retrieval from LANDSAT TM 5. *Remote Sensing of Environment*, 90: 434-440.

Stathopoulou, M., & Cartalis, C., 2007. Daytime urban heat islands from Landsat ETM+ and Corine land cover data: an application to major cities in Greece. *Solar Energy*, 81, pp. 358-368.

Synder, W. C., Wan, Z., Zhang, Y., & Feng, Y. Z., 1990. Classification-based emissivity for land surface temperature measurement from space. *International Journal of Remote Sensing*, 19(14), pp. 2753-2774.

Van, D., Griend, A. A., & Owe, M., 1993. On the relationship between thermal emissivity and the normalized difference vegetation index for natural surfaces. *International Journal of Remote Sensing*, 14(6), pp. 1119-1131.

Wan, Z., & Dozier, J., 1996. A generalized split-window algorithm for retrieving land surface temperature measurement from space. *IEEE Transaction on Geoscience and Remote Sensing*, 34, pp.892-905.

- Walson K. 1992. Two methods for measuring emissivity. *Remote Sensing of Environment*, 42, pp. 117-121.
- Xia, X. Q., Tian, Q. J., & Du, F. L., 2004. Analysis of Hyperspectral remote sensing images using a simplex method. *Journal of Image and Graphics*, 9(12), pp. 1487-1491.
- Yamaguchi, Y., Kahle, A. B., Tsu, H., Kawakami, T., & Pniel, M., 1998. Overview of Advanced Spaceborne Thermal emission and reflection radiometer (ASTER). *IEEE Transaction on Geoscience and Remote Sensing*, 36, pp. 1062-1071.
- Yuan, F., & Bauer, M. E., 2007. Comparison of impervious surface area and normalized difference vegetation index as indicators of surface urban heat island effects in Landsat imagery. *Remote Sensing of Environment*, 106, pp. 375-386.
- Zhou, J., Chen, Y. H., Zhang, J. S., Li, J., 2007. Urban impervious surface abundance estimation in Beijing based on remote sensing. *Remote Sensing for Land & resources*, 3(73), pp. 13-17.
- Tian, G., 2006. *Thermal Remote Sensing*. Publishing House of Electronics Industry. Beijing, China.
- Gillespie, A. R., Rokugawa, S. R., Hook, S. J., Matsunaga, T., & Kahle, A. B., 1999. Temperature/Emissivity Separation Algorithm Theoretical Basis Document, Version 2.4. <http://asterweb.jpl.nasa.gov/documents.asp>.

